Effect of Elastomer Type and Functionality on the Behavior of Toughened Polyamide Nanocomposites

I. Kelnar, J. Kotek, L. Kaprálková, J. Hromádková, J. Kratochvíl

Institute of Macromolecular Chemistry, Academy of Sciences of the Czech Republic, Heyrovsky Square 2, 162 06 Prague, Czech Republic

Received 24 March 2005; accepted 15 September 2005
DOI 10.1002/app.23644
Published online in Wiley InterScience (www.interscience.wiley.com).

ABSTRACT: The only shortcoming of PA6-based nanocomposites is low toughness, which is the same as that of the matrix. This work is focused on optimization of toughening these nanocomposites by introduction of small amounts of finely dispersed elastomers. A comparison of reactively compatibilized and analogous nonreactive elastomer-containing nanocomposites indicates the best-balanced mechanical behavior for polar nonreactive elastomers such as NBR and E-MA. This is explained by a significant compatibilizing effect of clay. Besides the elastomer particle size and its properties, the clay localization and its degree of ordering in the interfacial region also significantly influenced mechanical properties of the system. © 2006 Wiley Periodicals, Inc. J Appl Polym Sci 100: 1571–1576, 2006

Key words: polyamides; nanocomposites; toughness

INTRODUCTION

Nanocomposites (NC) with polyamide 6 (PA6) matrix are typical examples of a significant enhancement of all material parameters by platelet-like clay.[1] The only property that is not enhanced but even decreased is toughness.[2,3] The molecular-scale interactions influencing the nanocomposite behavior probably reduce the formation of energy-absorbing sites, such as matrix ligaments with lower resistance to shear flow, leading to enhanced toughness of some composites containing rigid inorganic micron-sized particles.[4] Effective toughening usually occurs with a dispersed phase, both inorganic filler and elastomeric particles, of the size[5] above 100 nm. In the case of PA6 microcomposite, the mentioned layer with reduced resistance to shear flow is formed by α-crystals (parallel to the filler surface), showing high anisotropy[4] in plastic deformation. In nanocomposites, instead of α-form that occurs typically in neat PA6, the clay-induced, less stable γ-form also exists, with lamellae grown perpendicularly to montmorillonite sheets,[6,7] which is probably less favorable to toughening. The toughening mechanism mentioned earlier[4] also requires debonding at the interphase. Such phase separation has not been observed in nanocomposites; for example, a study dealing with AFM observation of fracture surfaces confirms strongly immobilized polymer chains on the clay surface.[8] As a result, toughness enhancement due to the presence of nano-clay was found only for nanocomposites with inherently brittle matrices like epoxy or polyester resins.[8,9] For epoxy-based nanocomposites, further enhancement of toughness was achieved by addition of liquid rubbers.[10] Liu et al.[11] have found an increase in toughness by addition of 10% of maleated PP to PA6 nanocomposite prepared by polymerization. Generally, toughness enhancement by addition of relatively high amounts of low-modulus polymers leads to a marked reduction in strength and stiffness.

Recently, we have found toughness enhancement of melt-mixed nanocomposite with PA6 matrix by addition of elastomer particles with an average size of 60 nm.[12] The reduction in other properties is negligible, because of the high effect of these ultrafine rubber particles, already at low (5%) content. Depending on both clay and EPR-MA contents, a material with very interesting balanced properties, inaccessible in other ways, can be obtained. For example, seven times higher toughness (relative to matrix), accompanied by elevated strength and stiffness, was obtained. At the same time, the nano-clay-induced γ-crystalline form is less stable in the presence of fine, reactively compatibilized rubber particles.[12] We have also demonstrated that a reactively formed compatibilizer decreases the overall crystallinity of PA6 in binary and ternary reactive blends.[13,14] Some recent studies indicate the ability of both particulate and platelet-type nanofillers to compatibilize immiscible polymer pairs.[15–17] Also, the possibility of bridging the phases by a filler with a

Correspondence to: Ivan Kelnar (kelnar@imc.cas.cz).
Contract grant sponsor: Grant Agency of the Czech Republic; contract grant number: 106/03/0679.

TABLE I
Mechanical Properties of NC Containing 5% of Elastomer and 5% Clay in Dependence on the Elastomer Type and Particle Size

Composition	σ_b (MPa)	E (MPa)	a_t (kJ m^{-2})	D[a] (nm)
PA6	74	1620	16.5	—
PA6/C30B	94	2580	15	—
PA6/C30B/EPR-MA	85	2230	45	60
PA6/C30B/EPR	83	2550	36	<1000
PA6/C30B/SEBS-MA	81.5	2185	41	70
PA6/C30B/SEBS	86.5	2560	44	280
PA6/C30B/E-MA-GMA	75.5	2025	33	<100
PA6/C30/E-MA	89	2370	38	180
PA6/C30B/NBR	85	2420	62	220

[a] Elastomer particle size.

high aspect ratio is proposed.[18] Unfortunately, these works did not include evaluation of mechanical behavior. The present work brings a more comprehensive insight into elastomer-containing (toughened) nanocomposites. It is focused on the compatibilizing ability of clay in dependence on elastomer structure and the dependence of mechanical properties on the resulting morphology.

EXPERIMENTAL

Materials

The following materials were used in our study: Cloisite 30B (Southern Clay Products, Inc.; Gonzales, TX) montmorillonite modified with alkylbis (2-hydroxyethyl)methylammonium chloride, the alkyl being derived from tallow (clay content 74 wt %); Cloisite C15 montmorillonite modified with dialkyldimethylammonium chloride, the alkyl being derived from hydrogenated tallow; Polyamide 6 (PA6) Ultramid B5 (M_n = 42,000), BASF; Maleated (0.6%) ethene–propene elastomer (EPR-MA), Exxelor 1801, Exxon Mobil (Ludwigshafen, Germany); Ethene–propene elastomer (EPR), Buna AP 331, (Degussa Hüls, Koln, Germany); Maleated (2%) styrene/ethane–butene/styrene copolymer (SEBS-MA), Kraton FX1901 (Ottignies-Louvain-La Neuve, Belgium); Styrene/ethene–butene/styrene copolymer (SEBS) Kraton G1652; Ethene (68%) methyl acrylate (28%) glycidyl methacrylate (8%) copolymer (E-MA-GMA) Lotader 8900, Atofina; Ethene–methyl acrylate (30%) copolymer (E-MA) Lotril 28MA07 (Carling, France); Hydrogenated butadiene–acrylonitrile copolymer (NBR), Breon N 33, Nippon Zeon (Takaoka, Japan).

Nanocomposite preparation

Prior to mixing, PA6 and clay were dried at 85 and 70°C, respectively, for 12 h in a vacuum oven. The blends were prepared by mixing the components in the W 50 EH chamber of a Brabender Plasti-Corder at 255°C and 45 rpm for 10 min. The material was immediately compression-molded at 250°C to form 1-mm-thick plates. Strips cut from these plates were used for preparation of dog-bone specimens (gauge length 40 mm) in a laboratory micro-injection molding machine (DSM). The barrel temperature was 265°C, and that of mold 80°C. The reported values of the clay content are wt % of Cloisite C30B and are not corrected for neat silicate content.

Testing

Tensile tests were carried out at 22°C, using an Instron 5800 apparatus at a crosshead speed of 20 mm/min. The stress-at-break, σ_b, elongation at break, ε_b, and Young's modulus, E, were evaluated. Corresponding variation coefficients do not exceed 2%, 15 and 5%, respectively.

Tensile impact strength, a_t, was measured with one-side notched specimens, using a Zwick hammer with an energy of 4 J (variation coefficient 10–15%).

Dynamic mechanical analysis (DMA) was made in the single cantilever mode using DMA DX04T apparatus.

A PerkinElmer Pyris 1 DSC apparatus was used for calorimetric measurements. Thermograms were scanned in the temperature interval 80–260°C at a heating rate of 10°C/min.

Morphological observations

Phase structure was observed using scanning electron microscopy (SEM) and cryo-fractured samples. The elastomer phases were etched with *n*-heptane for 1 h or with boiling xylene for 2 min. The size of dispersed particles was evaluated from their micrographs using a MINI MOP image analyzer (Kontron Co., Germany). For transmission electron microscope (TEM) observations, ultrathin (60 nm) sections were cut under liquid

N_2 from a stained (RuO_4 vapor for 90 min) sample using an Ultracut UCT (Leica) ultramicrotome.

Wide-angle X-ray diffraction patterns (WAXS) were obtained with a powder diffractometer HZG/4A (Freiberger Präzisionsmechanik GmbH, Germany) and monochromatic Cu Kα radiation.

RESULTS AND DISCUSSION

Effect of elastomer type and content

Results in Table I and Figure 1 indicate the highest toughness and balance of all properties for nanocomposites (NCs) containing nonreactive polar elastomers, namely NBR and E-MA. This is a difference from that of analogous ternary blends,[13,14] with the best toughness found for functionalized elastomers. The reason is the compatibilizing effect of clay (together with minor increase in viscosity), leading to the sufficiently fine size of polar elastomer particles (~200 nm). Such particles are undoubtedly more favorable for toughening than those with dimensions below 100 nm obtained with reactive elastomers. Even for nonpolar incompatible EPR, the toughness is relatively close to the EPR-MA value. Although the cavitation was found in the elongated neck for all samples (Fig. 2) indicating "usual" function of elastomers, the micromechanical processes under impact are expected to differ. This is supported by the differences in toughness [Fig. 1(a), Table I]. Important could be also the differences in matrix crystallinity and variation of interfacial parameters by different clay arrangement, as will be discussed below. More complex deformational behavior in clay-containing system is indicated in the case of methyl acrylate copolymers, when both enhanced (E-MA) and lowered (E-MA-GMA) toughnesses were accompanied by fair and low levels of strength and stiffness, respectively. Another unusual feature is also decrease in toughness [Fig. 1(a)] in the case of 5% EMA. Hence, a more detailed fracture-mechanical study of these systems is planned. The enhanced mechanical behavior of nonreactive polar elastomer-containing NC, in particular higher modulus and tensile strength, is more remarkable at higher elastomer concentrations, as is obvious from concentration dependences in Figure 1. A similar decrease in modulus and strength was also found for reactive elastomer-containing blends with PA6 matrix, as a consequence of lowering the α-crystalline phase content by the presence of reactively formed copolymers[13]. Results obtained by WAXS study of NC shows almost no differences in the crystalline phase content and type. Similar results were obtained using DSC. The only effect observed was a slightly enhanced γ phase content (on expense of α crystallinity) in the case of E-MA shown in Figure 3. Generally, the crystallinity of NC is less affected by reactive compatibilization.

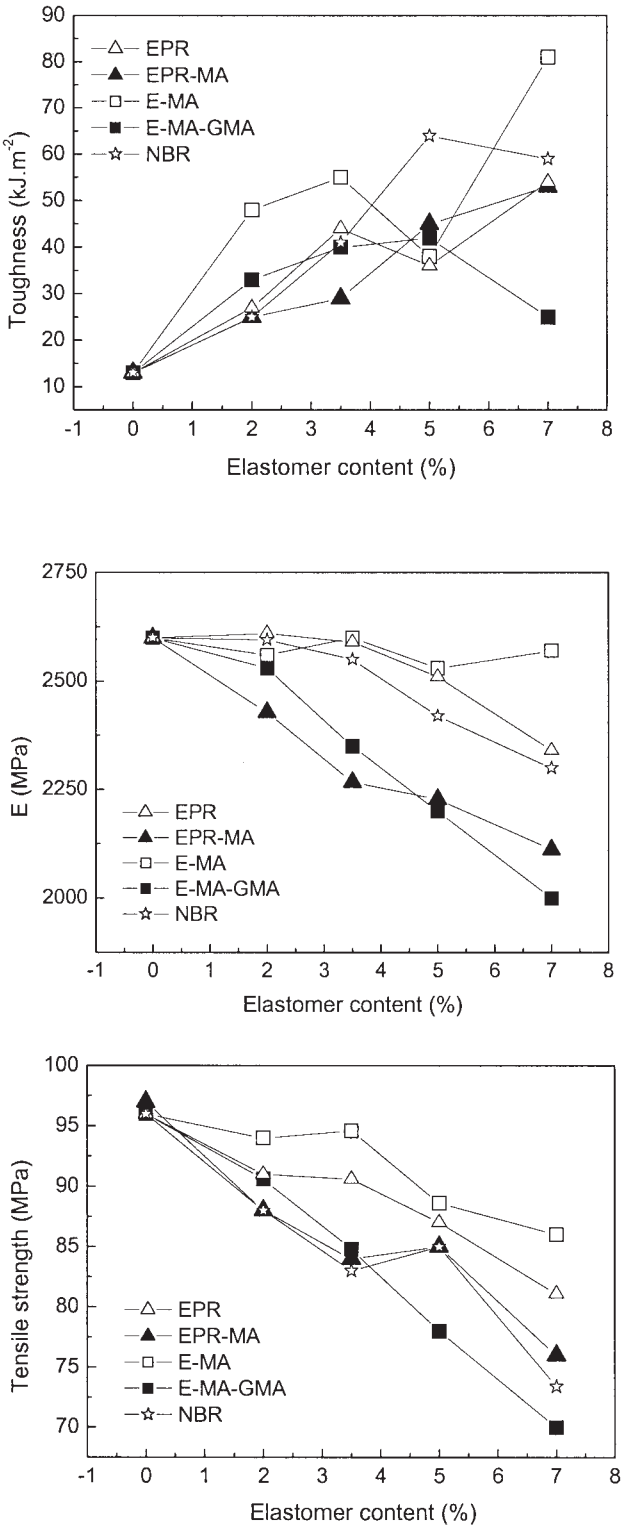

Figure 1 Mechanical properties of nanocomposite containing 5% of clay in dependence on the elastomer type end content.

Though the enhanced γ phase content may contribute to enhanced toughness,[19] its presence should deteriorate stiffness. As mentioned above [Table I, Fig. 1] the EMA- containing NC possess both enhanced

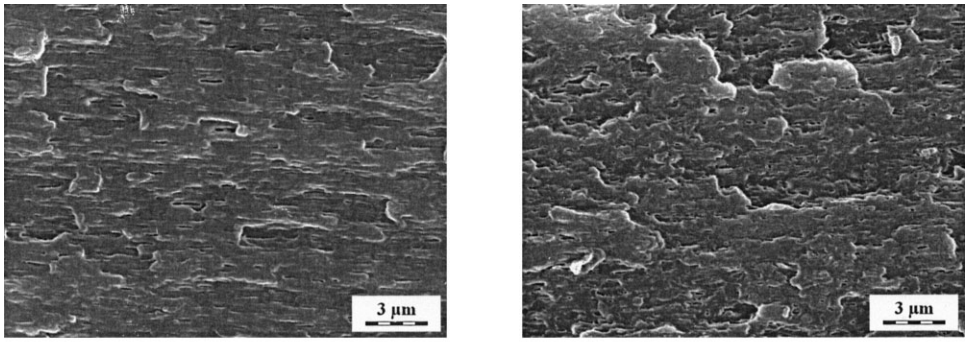

a) E-MA b) E-MA-GMA

Figure 2 Structure of elongated neck of nanocomposites containing 5% of elastomer.

strength and stiffness. Therefore, the deformational behavior is more affected by different arrangement of clay in the vicinity of elastomer (and thus parameters of the interface) as shown in the next chapter. The differences in structure and properties of the interfacial area are indicated also by slight differences in the course of thermal dependence of loss and storage moduli between reactive and nonreactive elastomer-containing NC, Figure 4.

Morphology

The differences in clay localization in the interfacial area were confirmed by TEM observations [Fig. 5(a–e)]. The morphology of the interface obviously depends on both elastomer polarity and reactivity; symmetric homogeneous "embedding" of elastomer by clay is more significant for polar elastomers like NBR [Fig. 5(a)]. Regularity of this clay layer decreases with lower polarity, as it is clear for E-MA [Fig. 5(b)]. For nonpolar EPR, an unchanged structure of exfoliated MMT around rubber occurs [Fig. 5(c)]. On the other hand, the presence of reactively formed copolymer suppresses the exfoliation in and near the interfacial area, like in E-MA-GMA [Fig. 3(d)] with less delaminated stacks of clay platelets. Similar morphology was found also for SEBS-MA (not shown). Surprisingly, elastomer particles surrounded by single platelets de-

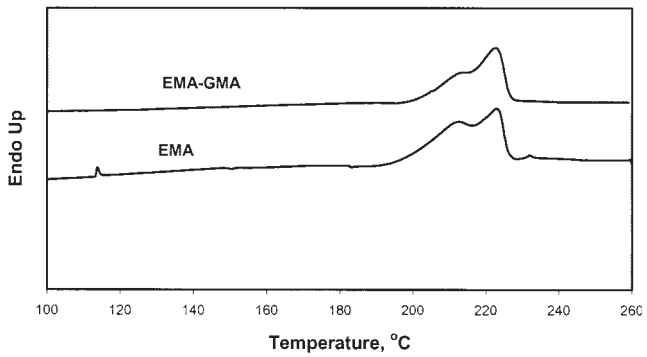

Figure 3 DSC heating scans of NC containing nonreactive and functionalized elastomer.

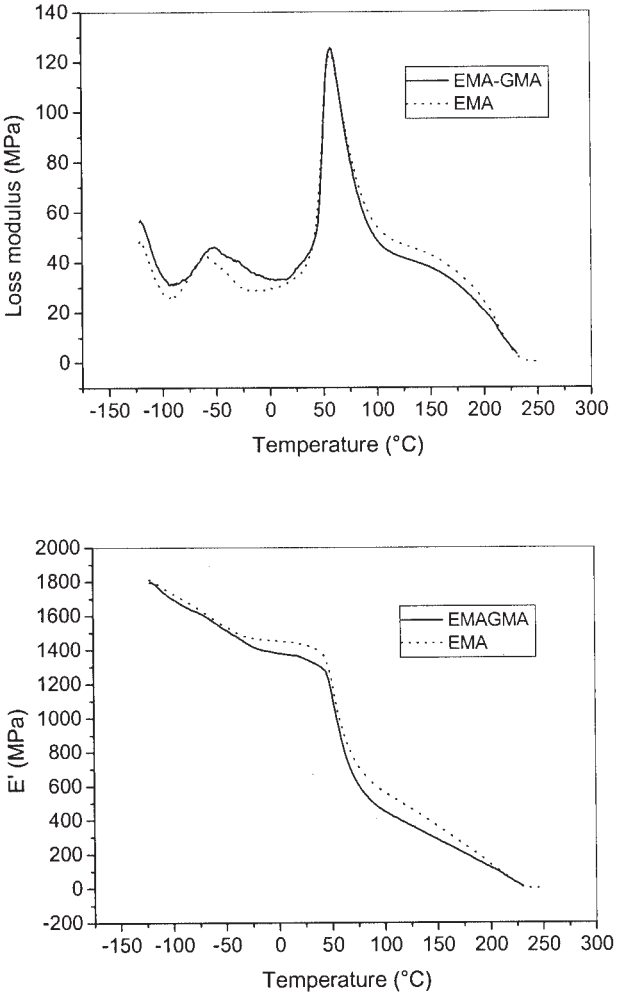

Figure 4 Thermal dependence of loss and storage modulus for nanocomposite containing 5% clay and 5% of reactive (EMA-GMA) and an analogous nonreactive elastomer (EMA).

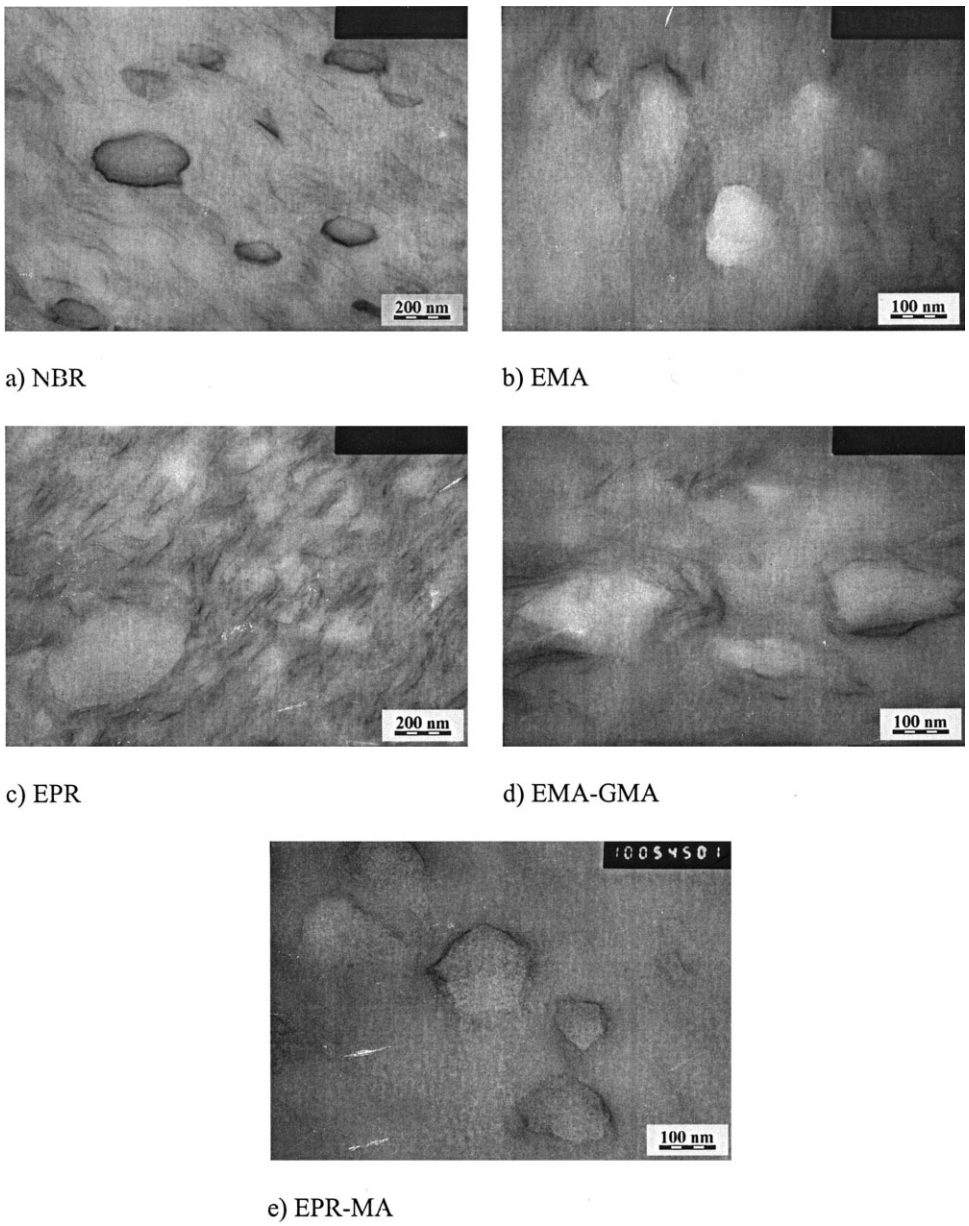

Figure 5 TEM observation of nanocomposites containing 5% of various elastomers.

termining their shape, were observed for EPR-MA [Fig. 5(e)]. Additionally, for all the elastomers used, clay platelets were not present inside elastomer particles. Generally, reduced delamination of clay due to the presence of reactively formed copolymer may be the reason for lower strength and stiffness of reactive elastomer containing NC. The corresponding variation of matrix parameters together with the above-mentioned (less favorable) low elastomer particle size is undoubtedly the reason for their lower toughness. For EPR-MA, the surrounding of its fine domains by clay [Fig. 3(e)] may suppress cavitation. To evaluate the impact of the observed structures on mechanical behavior, in particular toughness, a more comprehensive study (including NMR and AFM), also including expected minor changes in crystallinity, is necessary.

Effect of clay content

Figure 6(a–c) demonstrates the effect of increased clay concentration on behavior of an NC containing 5% of elastomer. Similarly to the above elastomer-concentration dependences (Fig. 1), a very fair balance of properties for NC containing nonreactive polar elastomers (NBR, E-MA) is found in the whole range of clay contents. In the case of E-MA containing NC, the strength and modulus are quite comparable with single NC values. Of interest is the even enhancement of toughness of PA6/elastomer combination by addition of a small amount (1%) of C30B, showing certain synergistic influencing of components. The significantly higher toughness of NC containg only 3.5% of E-MA [and showing also a different dependence on

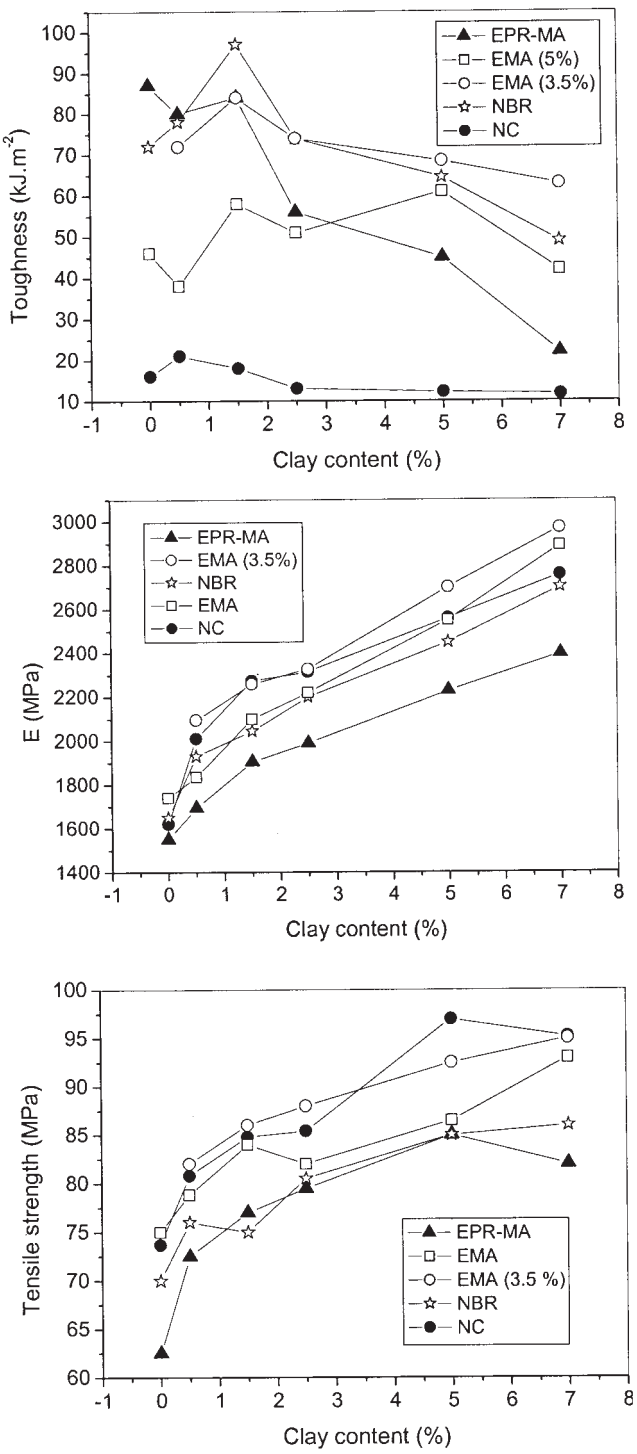

Figure 6 Dependence of mechanical properties of nanocomposite containing 5% of elastomer on the clay content.

the clay content Fig. 6(a)] in comparison with higher (5%) content indicate different deformational (energy-absorbing) behavior of NC compared with binary PA6/elastomer blends. Because of a clearly more complex effect of both dispersed components on the system behavior, a more thorough study of its dynamics using solid-state NMR[20] and characterization of crystallinity are planned.

CONCLUSIONS

The best-balanced mechanical behavior was found for nanocomposite containing finely dispersed nonreactive polar elastomers. Because of a very low dependence of the PA6 matrix crystallinity on the elastomer type, the reason is a more favorable phase structure with both elastomer particle size and arrangement of clay around them. Lower mechanical behavior for NC with reactive elastomers is a consequence of a negative effect of the *in situ* formed copolymer on clay exfoliation, predominantly near the interface. The presented results indicate that clay platelets affect mechanical behavior of the multiphase system both by the compatibilizing effect and by different localization and degree of exfoliation in the interfacial region.

References

1. Pinnavaia, T. J.; Beall, G. W., (Eds.). Polymer-Clay Nanocomposites; Wiley: New York, 2001.
2. Jimenez, G.; Ogata, N.; Kavai, H.; Ogihara, T. J Appl Polym Sci 1997, 64, 2211.
3. Fornes, T. D.; Yoon, P. J.; Keskkula, H.; Paul, D. R. Polymer 2001, 42, 9929.
4. Bartczak, Z.; Argon, A. S.; Cohen, R. E.; Kowaleski, T. Polymer 1999, 40, 2367.
5. Bucknall, C. B. Toughened Plastics; Applied Science Publishers: London, 1977.
6. Lincoln, D. M.; Vaia, R. A.; Wang, Z.-G.; Hsiao, B. S.; Krishnamoorti, R. Polymer 2001, 42, 9975.
7. Zerda, A. S.; Lesser, A. J. J Polym Sci Part B: Polym Phys 2001, 39, 1137.
8. Kordmann, X.; Berglund, L. A.; Sterte, J.; Giannelis, E. P. Polym Eng Sci 1998, 38, 1351.
9. Kojima, Y.; Usuki, A.; Kawasumi, M.; Okada, A.; Fukushima, Y.; Kurauchi, T.; Kamigaito, O. J Mater Res 1993, 8, 1185.
10. Isik, I.; Yilmazer, U.; Bayram, G. Polymer 2003, 44, 6371.
11. Liu, X.; Wu, Q.; Berglund, L. A.; Fan, J.; Qi, Z. Polymer 2001, 42, 8235.
12. Kelnar, I.; Kotek, J.; Munteanu, B. S.; Kaprálková, L. J Appl Polym Sci 2005, 96, 288.
13. Kelnar, I.; Stephan, M.; Jakisch, L.; Fortelný, I. J Appl Polym Sci 1997, 66, 555.
14. Kelnar, I.; Stephan, M.; Jakisch, L.; Fortelný, I. J Appl Polym Sci 2000, 78, 1597.
15. Gelfer, M. Y.; Song, H. H.; Liu, L.; Hsiao, B. S.; Chu, B.; Rafailovich, M.; Si, M.; Zaitsev, V. J Polym Sci Part B: Polym Phys 2003, 41, 44.
16. Voulgaris, D.; Petridis, D. Polymer 2002, 43, 2213.
17. Wang, S.; Hu, Y.; Song, L.; Liu, J.; Chen, Z.; Fan, W. J Appl Polym Sci 2004, 91, 1457.
18. Wan, Ch. Y.; Zhang, Y.; Zhang, Y. X.; Qiao, X. Y.; Teng, G. M. J Polym Sci Part B: Polym Phys 2004, 42, 286.
19. Mizuochi, I. M.; Kanamoto, K. Polymer 1998, 39, 4593.
20. Brus, J.; Kelnar, I.; Kotek, J. Macromolecules, to appear.